Pergamon

Int. J. Heat Mass Transfer. Vol. 38, No. 1, pp. 31–38, 1995
Copyright © 1994 Elsevier Science Ltd
Printed in Great Britain. All rights reserved
0017–9310/95 $9.50+0.00

0017–9310(94)00145–6

Effect of stress acting upon the solid network in the two-phase zone during solidification

Q. YU, M. MAKHLOUF and D. APELIAN
Department of Mechanical Engineering, Worcester Polytechnic Institute, Worcester, MA 01609, U.S.A.

(*Received* 10 *January* 1994 *and in final form* 13 *May* 1994)

Abstract—Having taken the solid network movement in the two-phase zone into consideration, this paper develops the original local solute redistribution equation. The additional term $\mathrm{div}\,V_S'$ in the new equation is dependent on the history of an effective stress σ' acting upon the solid network. The solidifying isotherm advances quickly and there is not enough time to make the solid network compressible at large cooling rates. With decreasing cooling rate, movement of the isotherm is gradually slowed and there is enough time to make the network deformed. It is suggested that the compressibility due to the normal stress may produce "channel space" filled by unstable flow under the conditions of small cooling rate during solidification. The calculated results have demonstrated that the back-flow toward the centerline increases when the stress is considered.

1. INTRODUCTION

It has been established both theoretically and experimentally that some defects that occur in a solidifying metal alloy, such as porosity, segregation, and hot tear, are related to interdendritic fluid flow in the two-phase zone of the alloy. The driving forces producing the interdendritic fluid flow, as a rule, include siphonic force due to solidification shrinkage (or expansion) and gravity acting on a fluid of variable density [1–8]. Under certain conditions, solid contraction and movement in the two-phase zone should also be considered as a driving force. It is generally believed that the solid contraction and movement affect the interdendritic fluid flow when the solid crystals in the two-phase zone form a network. In his analysis of the feeding mechanism in a solidifying casting, Campbell [9, 10] proposed that, during interdendritic feeding, the shrinkage pressure could become so high that the solid dendritic network and the solid outer shell of the casting also start to deform under the internal suction effect, and the hydrostatic tensions in metal alloys were evaluated theoretically considering the viscous flow of residual liquid and the general plastic collapse of the casting. Flemings [11] pointed out in research on dendritic solidification of semi-solid metals that strains with resulting liquid flow resulted in localized regions of macrosegregation in actual castings and ingots, and centerline segregation in continuous casting could be visualized as having a similar root cause, resulting from thermal contraction of the solid, accentuated by "bulging" of the casting due to the metallostatic head.

Quantitative descriptions of the interdendritic fluid flow are generally based on Darcy's equation and the local solute redistribution equation [1, 2]. A further mathematical model of convection in the two-phase zone, that accounts for momentum, heat and species transport in a multiphase and multiconstituent system, has recently been addressed. In this paper the local solute redistribution equation is developed with principles from the general model proposed by Bennon and Incropera [12, 13].

Assumptions for the local solute redistribution equation have generally been as follows [1, 6]:

(1) a small volume element in the two-phase zone is large enough that the fraction solid within it at any time is exactly the local average, but small enough that it can be treated as a differential element;
(2) there is no movement of the solid phase into or out of the element;
(3) solute enters or leaves the element only by liquid flow to feed shrinkage;
(4) mass flow in or out of the element by diffusion is merged into the fluid flow;
(5) solidification occurs with equilibrium at the solid–liquid interface so that there is no undercooling, and the rate of solidification is controlled only by the rate of heat transfer and convection within the two-phase zone;
(6) the local temperature and the composition of the solid at the interface are specified by the local composition of the liquid;
(7) diffusion in the solid is negligible;
(8) solid density is constant;
(9) no pore forms during solidification.

The purpose of this work is to relax assumptions (2) and (3). Movement of the solid phase in the two-phase zone and movement of the solute into or out of the element by liquid flow and by solid movement will

NOMENCLATURE

a_E	constant in equation (21b) [m]
b_{Ex}	constant in equation (21b) [m s^{-q}]
b_{Lx}	constant in equation (21a) [m s^{-q}]
$\bar{C}$	local average concentration [wt%]
C_L	liquid concentration [wt%]
C_S	local solid concentration [wt%]
$\bar{C}_S$	local average solid concentration [wt%]
E	Young's modulus [N m^{-2}]
g	gravity acceleration [m s^{-2}]
g_L	volume fraction liquid
g_S	volume fraction solid
k	equilibrium partition ratio
K	permeability [m^2]
L	length of ingot [m]
m	solid–solid contact coefficient
p	pressure [N m^{-2}]
P_0	ambient pressure [N m^{-2}]
q	constant in equation (21)
t	time [s]
T	temperature [°C]
T_E	eutectic temperature [°C]
T_L	liquidus temperature [°C]
U_b	volume of an element in two-phase zone [m^3]
U_E	velocity of the eutectic isotherm [m s^{-1}]

V	velocity of two-phase zone [m s^{-1}]
V_L	liquid velocity in two-phase zone [m s^{-1}]
V_S	solid velocity in two-phase zone [m s^{-1}]
V_x	component of V in x-direction [m s^{-1}]
V_y	component of V in y-direction [m s^{-1}]
X_E	position of the eutectic isotherm [m]
X_L	position of the liquidus isotherm [m].

Greek symbols

α	compressibility coefficient [m^2 N^{-1}]
β	solidification shrinkage
γ	strain
ε	cooling rate [°C s^{-1}]
η	viscosity [N s m^{-2}]
ρ	average density [kg m^{-3}]
ρ_L	liquid density [kg m^{-3}]
ρ_{LO}	density of the liquid at the liquidus isotherm [kg m^{-3}]
ρ_{LE}	density of the eutectic liquid [kg m^{-3}]
ρ_S	solid density [kg m^{-3}]
ρ_{SE}	density of the eutectic solid [kg m^{-3}]
σ	total stress [N m^{-2}]
σ'	effective stress [N m^{-2}]
σ_S	solid stress [N m^{-2}].

be taken into consideration. It should be pointed out that movement of the solid phase is considered as deformation of the solid network after the grains in the two-phase zone form a coherent network.

2. DEVELOPMENT OF THE NEW EQUATION

The basic equation for describing the effect of solid movement on solute redistribution is developed on the basis of the models of the continuum approach to a porous medium. For solidification occurring in the volume element treated as a porous medium, in which liquid flow and solid movement occur, the mass conservation equation and the solute conservation equation should be given as

$$\frac{\partial\bar{\rho}}{\partial t} = -\nabla\cdot(\bar{\rho}V) \tag{1}$$

and

$$\frac{\partial(\bar{\rho}\bar{C})}{\partial t} = -\nabla\cdot(\bar{\rho}\bar{C}V) \tag{2}$$

respectively. For a two-phase zone of a binary alloy system, each term in equations (1) and (2) is weighted with volume fraction solid g_S and volume fraction liquid g_L, that is,

$$\bar{\rho} = g_S\rho_S+g_L\rho_L \tag{3}$$

$$\bar{\rho}V = g_S(\rho_S V_S)+g_L(\rho_L V_L) \tag{4}$$

$$\bar{\rho}\bar{C} = g_S(\rho_S C_S)+g_L(\rho_L C_L) \tag{5}$$

and

$$\bar{\rho}\bar{C}V = g_S(\rho_S C_S V_S)+g_L(\rho_L C_L V_L). \tag{6}$$

Combining equations (1)–(6) (see Appendix) yields a new equation for solute redistribution:

$$\frac{1}{g_L}\left[\frac{\partial g_L}{\partial t}-\mathrm{div}\,(g_S V_S)\right] = -\frac{1-\beta}{1-k}\left(1+\frac{V_L\cdot\nabla T}{\varepsilon}\right)\frac{1}{C_L}\frac{\partial C_L}{\partial t}. \tag{7}$$

In the analysis, assumptions (2) and (3) were relaxed, and the other assumptions used in developing the original local redistribution equation were maintained. Comparison of equation (7) to the original local redistribution equation, i.e. equation (8), shows that the term $1/g_L(\partial g_L/\partial t)$ in the original equation is replaced by the term $1/g_L[\partial g_L/\partial t\text{-div}\,(g_S V_S)]$ in the new equation:

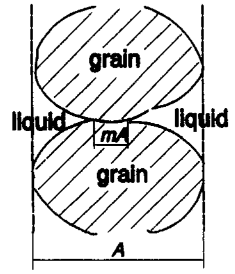

Fig. 1. Sketch of solid–solid contact in the two-phase zone.

$$\frac{1}{g_L}\frac{\partial g_L}{\partial t} = -\frac{1-\beta}{1-k}\left(1+\frac{V_L\cdot\nabla T}{\varepsilon}\right)\frac{1}{C_L}\frac{\partial C_L}{\partial t}. \tag{8}$$

3. ANALYSES OF THE NEW EQUATION

3.1. *Meaning of the new term*

In the left-hand side of equation (7), the term $\partial g_L/\partial t$ is a local derivative that represents the rate of change of the volume fraction liquid with time at a fixed point in the two-phase zone, and the term $\operatorname{div}(g_S V_S)$ is a new one. V_S is the velocity of deformation of the solid network at a point in the two-phase zone, and $g_S V_S$ is regarded as the solid velocity weighted by the volume fraction solid at the point. For convenience, there is

$$V'_S = g_S V_S. \tag{9}$$

The method proposed by Bear [14] is used to deal with the relationship between V'_S and effective stress acting upon the solid network. The term $\operatorname{div} V'_S$ in equation (7) is dependent on the history of the effective stress σ' acting upon the solid network:

$$\operatorname{div} V'_S = -\alpha\frac{d\sigma'}{dt}. \tag{10}$$

3.2. *The effective stress*

According to Terzaghi's theory [15], the total load of the solid–liquid two-phase zone is balanced by interparticle stress in the solid network and by pressure in the liquid phase. Taking into account the contact areas between the solid phase and liquid phase, as shown in Fig. 1, we may write

$$\sigma = (1-m)p + m\sigma_S. \tag{11}$$

The effective stress acting on the solid network, σ', may be defined as

$$\sigma' = m\sigma_S. \tag{12}$$

Typically, the range of g_S used in studying fluid flow in the two-phase zone is from 0.2 to 0.75. In this region, the liquid–solid contact area is larger than the solid–solid contact area, e.g. $m = 0.125$ at $g_S = 0.5$, so that $(1-m)p \cong p$. Thus equation (11) may be reduced to

$$\sigma = \sigma' + p. \tag{13}$$

In the above equations, a positive pressure ($p > 0$) means compression. Similarly, σ and σ' are taken as positive in the equations when they are compressive stresses.

In equation (12), the effective stress σ' is dependent on the solid–solid contact coefficient, m, which depends on the volume fraction solid for a certain casting structure such as equiaxed crystals. When g_S is small, i.e. less than 0.2–0.3, solidification of the alloy is mainly by mass feeding, and there is little contact among solid–phase grains in the two-phase zone; accordingly, m approaches zero. With increasing g_S, contact among them increases, and the value of m increases.

4. THE EFFECT OF STRESS ON FLUID FLOW

4.1. *Normal compressibility*

A fluid moving relative to a solid boundary exerts a force on that boundary. This force is caused by two factors. The first is a shear stress due to viscosity and velocity gradient at the boundary surface. This shear stress gives rise to a force tangential to the surface and causes slip in the solid network. The second is pressure variation along the surface that acts normal to the surface and causes compressibility of the solid network. Both slip and compressibility exist simultaneously in the solid network.

The slip due to shear stress and the compressibility due to normal stress, which are indicated not with a partial derivative, but with the total derivative in equation (10), make the solid-phase movement in the two-phase zone complicated. In order to simplify the problem, only the normal compressibility, i.e. compressibility due to the normal stress, is considered. Though this assumption should be considered an approximation, the main feature of the solid-phase movement may be emphasized. Since the shear stress acting on the solid network changes the relative positions among the solid phases, the initial deformation takes place as a result of slipping movement and readjustment of the solid phases. As the volume fraction solid increases, these movements decrease and, eventually, most of the deformation results from the compressibility of the zone associated with the solid network. When compressibility is taken into consideration, equation (10) is turned into [14]

$$\operatorname{div} V'_S = -\alpha\frac{\partial\sigma'}{\partial t} \tag{14}$$

where the total derivative of equation (10) is replaced by the partial derivative.

4.2. *Relationship of solid-phase movement with fluid flow*

For convenience, multiplying equation (7) by $\partial t/\partial T$ gives the new form

$$\left(\frac{\partial g_S}{\partial t} + \operatorname{div} V'_S\right)\frac{\partial t}{\partial T} = \left(\frac{1-\beta}{1-k}\frac{g_L}{C_L}\frac{\partial C_L}{\partial T}\right)\left(1+\frac{V_L\cdot\nabla T}{\varepsilon}\right) \tag{15}$$

where $\partial g_S/\partial t = -\partial g_L/\partial t$. The quantity inside the first bracket on the right-hand side of equation (15) is always negative, regardless of the value of k. According to prior studies [2], different cooling conditions of an ingot can cause three modes of fluid flow in the two-phase zone, i.e. stable flow, intermediate flow, and unstable flow. These modes are defined by the value of $(V_L \cdot \nabla T)/\varepsilon$: stable flow at $(V_L \cdot \nabla T)/\varepsilon > 0$; and unstable flow at $(V_L \cdot \nabla T)/\varepsilon < -1$. They are still used to analyze equation (7) here.

If only normal compressibility is taken into account, the left-hand side of equation (15) becomes†

$$\left(\frac{\partial g_S}{\partial t} + \mathrm{div}\, V_S'\right) = \frac{\partial g_S}{\partial T} + \frac{1}{U_b}\frac{\partial U_b}{\partial T}. \qquad (16)$$

With decreasing temperature, the volume of the two-phase zone U_b decreases due to the compressive effect of the effective stress acting upon the solid network, so there is always

$$\frac{\partial U_b}{\partial T} > 0. \qquad (17)$$

Two cases are discussed below.

Case a: *stable flow* $(V_L \cdot \nabla T)/\varepsilon > 0$. Since the right-hand side of equation (15) is less than zero at $(V_L \cdot \nabla T)/\varepsilon > 0$, there is

$$\frac{\partial g_S}{\partial T} + \frac{1}{U_b}\frac{\partial U_b}{\partial T} < 0$$

or

$$\frac{\partial g_S}{\partial T} < -\frac{1}{U_b}\frac{\partial U_b}{\partial T}. \qquad (18)$$

Now from equation (17):

$$\frac{\partial g_S}{\partial T} < 0 \qquad (19a)$$

$$\left|\frac{\partial g_S}{\partial T}\right| > \frac{1}{U_b}\frac{\partial U_b}{\partial T}. \qquad (19b)$$

Equation (19) shows that the volume fraction solid increases with decreasing temperature and that the variation of the volume fraction due to the solid-phase movement cannot play an effective role, i.e. the term $1/U_b(\partial U_b/\partial T)$ does not make the left-hand side of equation (15) less than zero. Accordingly, the flow remains stable.

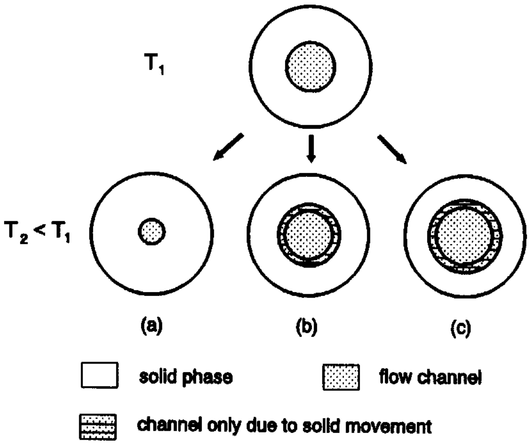

Fig. 2. Schematic illustration of influence of solid movement on change in flow channel: (a) stable flow; (b) unstable flow only, due to solid movement; (c) unstable flow due to natural convection and solid movement.

Case b: *unstable flow* $(V_L \cdot \nabla T)/\varepsilon < -1$. The right-hand side of equation (15) is greater than zero at $(V_L \cdot \nabla T)/\varepsilon < -1$, hence

$$\frac{\partial g_S}{\partial T} + \frac{1}{U_b}\frac{\partial U_b}{\partial T} > 0. \qquad (20)$$

Equation (20) indicates that the unstable flow may be caused by two terms: $\partial g_s/\partial T$ and $1/U_b(\partial U_b/\partial T)$. Since the term $1/U_b(\partial U_b/\partial T)$ is always positive during solidification, then $\partial g_s/\partial T$ may have either of two values: (1) $-1/U_b(\partial U_b/\partial T) < \partial g_S/\partial T \leqslant 0$, i.e. $\partial g_S/\partial T \leqslant 0$, which implies that the unstable flow in the two-phase zone is caused mainly by the solid-phase movement, that is, only the term $1/U_b(\partial U_b/\partial T)$ makes the left-hand side of equation (15) greater than zero; or (2) $\partial g_S/\partial T > 0$, which implies that the unstable flow is caused jointly by both the effective stress and the gravity force acting on a fluid with various densities.

Whether stable flow or unstable flow develops in the two-phase zone of the solidifying alloy depends on the cooling rate ε. For an Al–4.5 wt% Cu alloy, for example, stable flow occurs when $\varepsilon > 10^{-1}$ °C s^{-1} and unstable flow occurs when $\varepsilon < 10^{-2}$ °C s^{-1} [16]. The two-phase zone associated with the solid network can strain under the action of a definite stress. When the cooling rate is large, the solidifying isotherm advances fast and there is not enough time to produce the strain. This is the case shown with equation (18). It should be noted, however, that a residual stress may remain in the solidified ingot through the strain does not occur. When the cooling rate is small, the movement of the isotherm is slow, and the effective stress acting on the solid network may play a role in forming "channel space" that fills up with unstable fluid flow. Figure 2 is a schematic illustration of the effect of the solid-phase movement on the flow channel in a volume element for both cases: stable flow and unstable flow. Figure 2a depicts the case for stable flow where the solid-phase movement plays no role in forming the channel. Figure 2b depicts the case for unstable flow

---

† For a two-phase zone treated as a porous medium, the bulk volume of the element of the two-phase zone is U_b and velocity of the solid network in the element is V_S'. According to the concept of total derivative [14], there is

$$\mathrm{div}\, V_S' = \frac{1}{U_b}\frac{\mathrm{d}U_b}{\mathrm{d}t}.$$

For normal compressibility only, the above equation becomes

$$\mathrm{div}\, V_S' = \frac{1}{U_b}\frac{\partial U_b}{\partial t}.$$

due to solid-phase movement only. It should be understood that this case is merely theoretical because natural convection due to gravity always exists in the two-phase zone except for under microgravity conditions. In Fig. 2c, the unstable flow in the channel is caused by both the stress and by gravity acting on a fluid with variable density.

5. THE MODELS FOR CALCULATION AND THE COMPUTED RESULTS

5.1. *The solidification model and the temperature field*

The solidification model in this paper is schematically presented in Fig. 3, where there is a chill surface at each side of the mold and an insulated wall on its top and on its bottom. In what follows the model is used to investigate the effect of the stress on interdendritic fluid flow after a solid network has been formed in the two-phase zone of an alloy. The strain and stress due to solidification shrinkage are taken into consideration here.

It is convenient to specify the temperature field first, before the pressure field and the velocity field are calculated. The method used to specify the temperature field is mainly due to Maples and Poirier's work [6]. The positions of the liquidus and the eutectic isotherms are given by

$$|x_L(t)| = \frac{L}{2} - b_{Lx}t^q \tag{21a}$$

$$|x_E(t)| = \frac{L}{2} - b_{Ex}t^q - a_E. \tag{21b}$$

If temperature varies linearly across the mushy zone, the temperature field can be obtained from the equation below:

$$T(|x|, t) = T_E + \frac{(|x| - |x_E|)}{(|x_L| - |x_E|)}(T_L - T_E). \tag{22}$$

5.2. *The velocity equation and the pressure equation*

The velocity equation used to calculate the interdendritic fluid flow is based on Darcy's law [2], thus

$$V_L = -\frac{K}{\eta g_L}(\nabla p + \rho_L g). \tag{23}$$

In order to complete the calculation of the interdendritic fluid flow, the pressure equation in the two-phase zone was derived [6]:

$$\nabla^2 p + A \cdot \nabla p + B = 0 \tag{24}$$

where

$$A = \frac{\eta}{K}\nabla\left(\frac{K}{\eta}\right) - a\nabla T$$

$$B = \frac{\eta}{K}\nabla \cdot \left(\frac{K}{\eta}\rho_L g\right) + a\left(\frac{\eta}{K}g_L\frac{\partial T}{\partial t} - \rho_L g \cdot \nabla T\right)$$

$$a = \frac{\rho_L(\rho_L - \rho_S) - (1-k)\rho_S C_L \mathrm{d}\rho_L/\mathrm{d}C_L}{\rho_L(1-k)\rho_S C_L \mathrm{d}T/\mathrm{d}C_L}.$$

The boundary conditions for equation (24) are as follows. Since it is assumed that convection in the bulk liquid is negligible, then

$$p = p_0 + \rho_{L0}g(H - y)$$
$$\text{at} \quad x = |x_L| \quad \text{for} \quad 0 \leqslant y \leqslant H. \tag{25}$$

Since the top and the bottom of the two-phase zone in Fig. 3 are insulated, thus

$$V_y = 0 \quad \text{at} \quad y = 0 \quad \text{and} \quad y = H$$
$$\text{for} \quad |x_E| \leqslant |x| \leqslant |x_L|. \tag{26}$$

At the eutectic isotherm, there is a finite amount of liquid of eutectic composition which solidifies at a constant temperature. Since the densities of the eutectic-liquid and the eutectic-solid are not equal, there must be flow to compensate for solidification shrinkage (or expansion) of the eutectic. This requirement is

$$V_x = -\frac{\rho_{SE} - \rho_{LE}}{\rho_{LE}}U_E$$
$$\text{at} \quad x = |x_E| \quad \text{for} \quad 0 \leqslant y \leqslant H. \tag{27}$$

Equations (26) and (27) are rewritten to provide the boundary conditions for the pressure equation. Substituting equation (26) for V_y in equation (23) gives

$$\frac{\partial p}{\partial y} = -\rho_L g \quad \text{at} \quad y = 0 \quad \text{and} \quad y = H$$
$$\text{for} \quad |x_L| \leqslant |x| \leqslant |x_E| \tag{28a}$$

and substituting equation (27) for V_x in equation (23) gives

$$\frac{\partial p}{\partial x} = \frac{\eta g_L}{K}\frac{\rho_{SE} - \rho_{LE}}{\rho_{LE}}U_E$$
$$\text{at} \quad x = |x_E| \quad \text{for} \quad 0 \leqslant y \leqslant H. \tag{28b}$$

Also, at the centerline

$$\frac{\partial p}{\partial x} = 0. \tag{29}$$

5.3. *The effective stress*

As described earlier, during solidification a stress develops and acts on the solid network. The stress results from solidification shrinkage and solid contraction. The two-phase zone can not freely contract with decreasing temperature when the solid network appears in the whole zone, and there is a resistance to shrinkage of the two-phase zone. It is proposed that the stress and the strain be calculated by the models described below.

The solidification shrinkage β can be evaluated with the liquid and solid densities during solidification:

$$\beta = \frac{\rho_S - \rho_L}{\rho_S}. \tag{30}$$

Figure 4 shows liquid and solid densities for Al–4.5 wt% Cu alloy [2]. Since β is a volume contraction

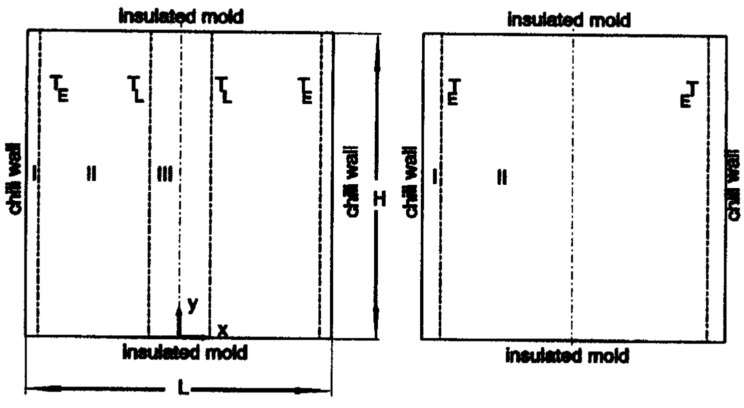

(a) (b)

Fig. 3. Solidification model: (a) before forming network; (b) after forming network; I, solid zone, II, two-phase zone; III, liquid zone.

percentage, the strain γ due to the shrinkage should be approximately

$$\gamma = \tfrac{1}{3}\beta. \tag{31}$$

The two-phase zone of a solidifying alloy is generally regarded as a body with visco-elastic-plastic behavior. The incorporation, however, of viscous processes into a model of the formation process leads to a great increase in the complexity of the problem. In consequence, a full visco-elastic-plastic model is not available at the present time. The following discussion, therefore, concentrates on the simpler treatment that considers the two-phase zone of the solidifying alloy as a Kelvin body with visco-elasticity, that is [17, 18],

$$\sigma_S = \eta\dot{\gamma} + E\gamma. \tag{32}$$

According to equation (12), the effective stress acting on the solid network is

$$\sigma' = m(\eta\dot{\gamma} + E\gamma) \tag{33}$$

where $m = g_S^3$ at $0.2 \leqslant g_S < 0.75$ and $m = 0$ at $g_S < 0.2$.

Figure 5(a) shows the calculated profile of interdendritic fluid flow in the two-phase zone of an alloy under the cooling condition of forming unstable flow, but without the action of the effective stress. Figure 5(b) shows the calculated profile with the action of the effective stress. It can be seen by comparison that the back-flow towards the centerline in Fig. 5(b) is larger than in Fig. 5(a). Figure 6 shows the dependence of the effective stress on the positions of x-coordinate for the different positions of y-coordinate when calculating the velocity profiles in Fig. 5(b).

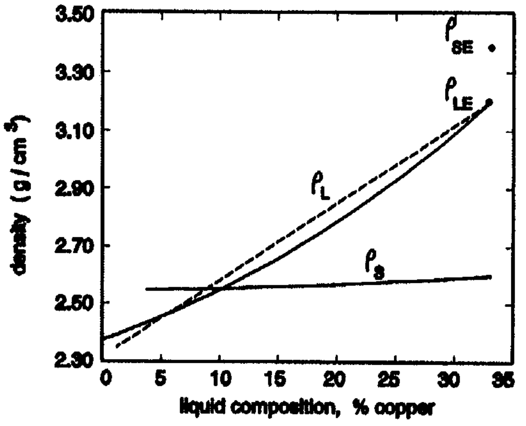

Fig. 4. Liquid and solid densities in two-phase zone of Al–4.5 wt% Cu alloy.

6. CONCLUSIONS

(1) When solid network movement in the two-phase zone is taken into consideration, the original local solute redistribution equation is expanded into equation (7), in which the term $1/g_L(\partial g_L/\partial t - \text{div } V_S')$ replaces the term $1/g_L(\partial g_L/\partial t)$ in the original equation. The divergence of the velocity field V_S' is dependent on the history of the effective stress σ' acting on the solid network.

(2) The effective stress σ' is directly proportional to the solid–solid contact coefficient m, which is dependent on the volume fraction solid g_S for a certain casting structure such as equiaxed crystal. With increasing g_S, the contacts among the solid-phase grains in the two-phase zone increase and the magnitude of σ' increases.

(3) Under fast cooling rates, the solidifying isotherm advances quickly and there is not enough time to make the solid network compressible. However, with decreasing cooling rate, the movement of the isotherm is slow and there may be enough time for the solid network to form. The unstable flow in the two-phase zone, which is caused by both the effective stress and the gravity force acting on a fluid with

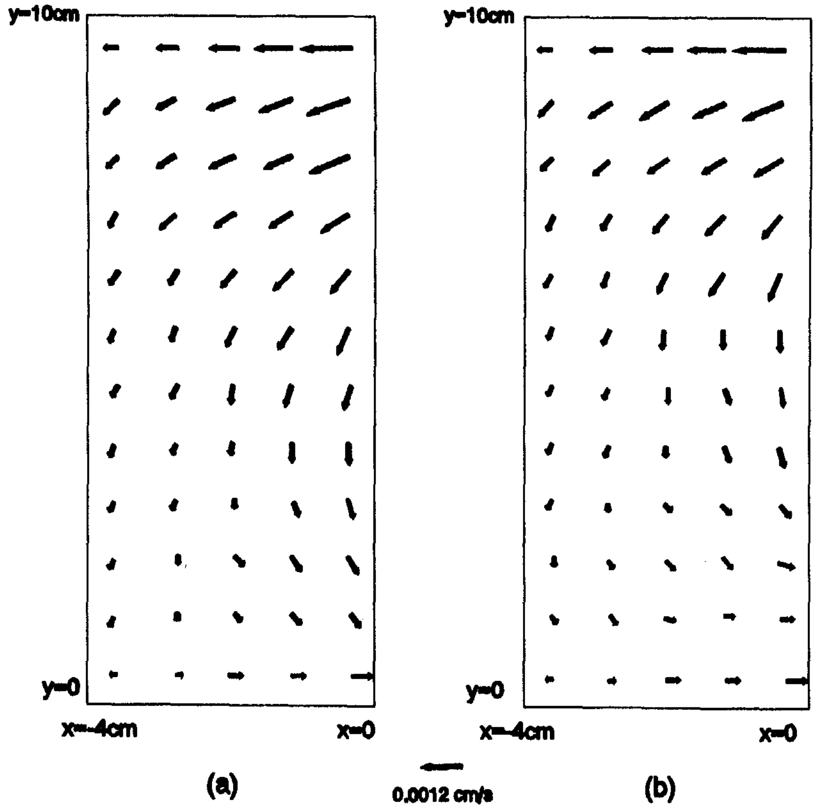

Fig. 5. Velocity profiles after forming network: (a) without action of stress, (b) with the action.

varying density, will fill the "channel space" formed by the network movement.

(4) The calculated velocity profiles show that the back-flow towards the centerline of the ingot when the effective stress is included in the analysis is larger than that when the effective stress is ignored.

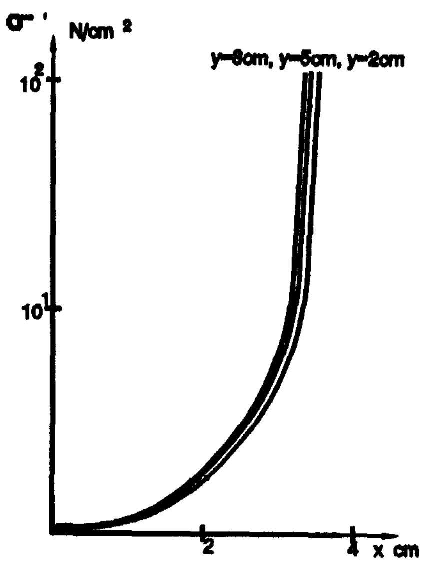

Fig. 6. Dependence of the effective stress on position of x at different positions of y.

REFERENCES

1. M. C. Flemings and G. E. Nereo, Macrosegregation Part 1, *Trans. AIME* **239**, 1449–1460 (1967).
2. R. Mehrabium, M. Keane and M. C. Flemings, Interdendritic fluid flow and macrosegregation; influence of gravity, *Metall. Trans.* **1**, 1209–1220 (1970).
3. A. Bejan and K. R. Khair, Heat and mass transfer by natural convection in a porous medium, *Int. J. Heat Mass Transfer* **28**, 909–918 (1985).
4. W. D. Bennon and F. P. Incropera, Numerical simulation of binary solidification in a vertical channel with thermal and solutal mixed convection, *Int. J. Heat Mass Transfer* **31**, 2147–2160 (1988).
5. D. Apelian, M. C. Flemings and R. Mehrabian, Specific permeability of partially solidified dendritic networks of Al–Si alloys, *Metall. Trans.* **5**, 2533–2537 (1974).
6. L. Maples and D. R. Poirier, Convection in the two-phase zone of solidifying alloys, *Metall. Trans.* **15B**, 163–172 (1984).
7. Q. Yu and Y. Zhou, Numerical simulation of convection in the two-phase zone of a binary alloy, *Int. J. Heat Mass Transfer* **34**, 843–852 (1991).
8. S. D. Felicelli, J. C. Heinrich and D. R. Poirier, Simulation of freckles during vertical solidification of binary alloys, *Metall. Trans.* **22B**, 847–859 (1991).
9. J. Campbell, Hydrostatic tensions in solidifying alloys, *Trans. AIME* **242**, 268–271 (1968).
10. J. Campbell, On the origin of porosity in long freezing range alloys, *Brit. Foundryman* 147–158 (April 1969).

11. M. C. Flemings, Behavior of metal alloys in the semisolid state, *Metall. Trans.* **22A,** 957–981 (1991).
12. W. D. Bennon and F. P. Incropera, A continuum model for momentum, heat and species transport in binary solid–liquid phase change systems, 1. Model formulation, *Int. J. Heat Mass Transfer* **30,** 2161–2170 (1987).
13. W. D. Bennon and F. P. Incropera, A continuum model for momentum, heat and species transport in binary solid–liquid phase change systems, 2. Application to solidification in rectangular cavity, *Int. J. Heat Mass Transfer* **30,** 2171–2187 (1987).
14. J. Bear, *Dynamics of Fluids in Porous Media.* American Elsevier, New York (1972).
15. K. Terzaghi, *From Theory to Practice in Soil Mechanics.* Wiley, New York (1960).
16. Q. Yu and Y. Zhou, Influence of mould rotation on macrosegregation in ingot, *Acta Metall. Sin.* (*Engng Edn*) *Ser.* **B2,** 81–86 (1989).
17. F. S. Sherman, *Viscous Flow.* McGraw-Hill, New York (1990).
18. A. J. Fletcher, *Thermal Stress and Strain Generation in Heat Treatment.* Elsevier, London (1989).

APPENDIX: DERIVATION OF EQUATION (7)

For ρ_S = constant, substituting equation (6) into equation (2) and expanding the right-hand side of equations (2) provide

$$\frac{\partial(\bar{\rho}\bar{C})}{\partial t} = -\rho_S\bar{C}_S\nabla\cdot(g_S V_S) - g_L\rho_L V_L\cdot\nabla C_L - C_L\nabla\cdot g_L\rho_L V_L \tag{A1}$$

or substituting equation (1) into equation (A1)

$$\frac{\partial(\bar{\rho}\bar{C})}{\partial t} = -\rho_S(\bar{C}_S - C_L)\nabla\cdot(g_S V_S) + C_L\frac{\partial\bar{\rho}}{\partial t} - g_L\rho_L V_L\cdot\nabla C_L. \tag{A2}$$

From equations (3) and (5), the left-hand sides of equations (1) and (2) can be expressed as

$$\frac{\partial\bar{\rho}}{\partial t} = \frac{\partial}{\partial t}(g_S\rho_S + g_L\rho_L) \tag{A3}$$

and

$$\frac{\partial(\bar{\rho}\bar{C})}{\partial t} = \frac{\partial}{\partial t}(g_S\rho_S\bar{C}_S + g_L\rho_L C_L). \tag{A4}$$

Since assumptions (5), (7), and (8) still exist now, that is, the equilibrium partition ratio k applies at the liquid–solid interface, there is no diffusion in the solid, and ρ_S = constant during solidification, then [1]

$$\frac{\partial}{\partial t}(g_S\rho_S\bar{C}_S) = kC_L\rho_S\frac{\partial g_S}{\partial t}. \tag{A5}$$

Substituting equations (A3)–(A5) into (A2) and rearranging,

$$\rho_S C_L(1-k)\left[\frac{\partial g_S}{\partial t} + \nabla\cdot(g_S V_S)\right] = g_L\rho_L\frac{\partial C_L}{\partial t} + g_L\rho_L V_L\cdot\nabla C_L. \tag{A6}$$

If C_L depends only on temperature and hence on position and time, an expression describing movement of isoconcentrations and isotherms is

$$-\frac{\varepsilon}{\nabla T} = -\frac{\partial C_L/\mathrm{d}t}{\nabla C_L} \tag{A7}$$

when no pores form, i.e. $g_L + g_S = 1$ or $\partial g_L = -\partial g_S$, and $\beta = (\rho_S - \rho_L)/\rho_S$. Combining equations (A6) and (A7) gives equation (7).